

Sensitivity Analysis of Closest Point of Approach

Ying Huo, Daniel Delahaye, Yanjun Wang

► **To cite this version:**

Ying Huo, Daniel Delahaye, Yanjun Wang. Sensitivity Analysis of Closest Point of Approach. ICRAAT 2018, 8th International Conference for Research in Air Transportation, Jun 2018, Barcelone, Spain. hal-01823194

HAL Id: hal-01823194

<https://hal-enac.archives-ouvertes.fr/hal-01823194>

Submitted on 25 Jun 2018

HAL is a multi-disciplinary open access archive for the deposit and dissemination of scientific research documents, whether they are published or not. The documents may come from teaching and research institutions in France or abroad, or from public or private research centers.

L'archive ouverte pluridisciplinaire **HAL**, est destinée au dépôt et à la diffusion de documents scientifiques de niveau recherche, publiés ou non, émanant des établissements d'enseignement et de recherche français ou étrangers, des laboratoires publics ou privés.

Sensitivity Analysis of Closest Point of Approach

Ying HUO
OPTIM-Team/ENAC-LAB
ENAC – Université de Toulouse
Toulouse France

Daniel DELAHAYE
OPTIM-Team/ENAC-LAB
ENAC – Université de Toulouse
Toulouse France

YanJun WANG
College of Civil Aviation
NUAA
Nanjing China

Abstract—The increase of air traffic demand leads to a higher risk of collision. In the process of ensuring the safety of air traffic, Closest Point of Approach (CPA) plays an important role in estimating potential dangers. Sensitivity analysis of CPA provides related information about the influences from different aircraft parameters to CPA. The parameters such as speed of aircraft, flight direction and relative position of aircraft are used as inputs, the closest distance between two aircraft and the time from the first observation to CPA are considered to be the outputs. The main idea presented in this paper includes the establishment of the model and the selection of sensitivity analysis method. The proposed model contains all possible encounter scenarios of two aircraft and can establish the relations between dependent and independent variables simply. The objective of sensitivity analysis is to detect the influential effects from the inputs to the outputs based on the model. Thus two methods are considered in this paper: Local approach uses the partial derivative corresponding to a specific point with respect to a certain input to determine the sensitivity. This method is limited by explaining one situation each time. Variance-based method which is under a probabilistic framework bases on random numerical sampling generates numerical results to determine the global influential effects with certain assumptions. The sensitivity analysis will benefit air traffic management controllers by offering auxiliary strategies while a dangerous situation occurs.

Keywords—Closest point of approach, sensitivity analysis, local approach, variance-based method

I. INTRODUCTION

The increase of air traffic has potential impact on the collision risk between aircraft. Recently, not only commercial air transportation but general aviation transportation grow dramatically which result in heavy workload for air traffic controllers and higher risk of accidents. The widely used Traffic Collision Avoiding System (TCAS) and Airborne Collision Avoiding System (ACAS) play important roles in avoiding the potential collisions between aircraft and obstacles, as well as providing solutions to air crew for emergency situations. Since in en-route segment, the separation between two aircraft is the primary consideration of the collision avoidance system, it is necessary to investigate Closest Point of Approach (CPA) to determine the closest distance under the potential collision scenarios in the free airspace[1].

During the process of developing collision detection and avoidance system, lots of research works based on CPA are studied. A typical one is given by Kuchar and Yang on the conflict detection model [2]. Usually the mathematical part of resolution advisory detection ends up with computational formula of CPA [3].

Sensitivity analysis has been widely employed for various kinds of problems to determine the influential effects between the inputs and the outputs [4]. Houck and Powell have studied the sensitivity of collision risk on parallel approach by using a runway reference frame. A baseline case was used as a criterion to analyze the relationship between variables such as roll rate, heading change, air speed etc. and the output which is collision rates by applying the least square method [5]. Jackson and Zhao defined the modeling error between predicted trajectories and real trajectories which are fed back by pilots. Except the modeling errors and human mistakes, the linearly related equation between predicted trajectories and real trajectories can be used to determine the expressions for closed-loop sensitivity [6]. These previous work use different kinds of methods to achieve the final goal of sensitivity analysis on the specific aspects.

Although there are plenty of studies related to CPA, the contributions from the parameters which determine the time and distance to CPA has been less addressed. In this paper we present the sensitivity analysis of CPA considering only two converging aircraft. The study is based on flight cruise phase when aircraft speed, heading, and altitude do not change. A preliminary analysis on CPA is conducted to detect the time and the distance between initial observation at time t_0 and the closest point at time t_{cpa} . Then, a model is developed which takes all the possible scenarios into account. Therefore, the information we extract from radar data can be adapted to one of the scenarios in the model.

The structure of this paper is organized as follows. Section II provides the background information on CPA and introduces the parameters that will be used as inputs and outputs. Modeling process is also presented in this section. Section III using local approach for sensitivity analysis, results are represented with figures. Section IV presents the process of using global sensitivity analysis method including the calculation of sensitivity indices. Simulation and results of this method are explained. In section V, we conclude the work and sketches the further direction of research.

II. CLOSEST POINT OF APPROACH

A. Definition

Closest Point of Approach represents to the positions of two dynamically moving objects where they reach their closest distance [7].

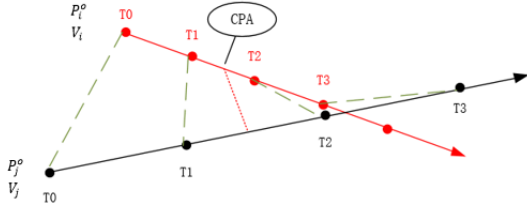


Figure 1. The CPA obtained by two objects moving with different speeds

Fig. 1 shows an example of CPA with two moving objects. V_i , P_i^o are the speed vector and the initial position of aircraft i , while V_j , P_j^o are linked to aircraft j . As they are flying with different speeds and directions, the distance between these two aircraft first decreases and then increases. For all the situations we can locate the time t_{cpa} when the distance between them is minimum.

Two parameters T_{CPA} and D_{CPA} are introduced to represent the outputs. For two aircraft, T_{CPA} is the time from the initial position to the closest point, i.e. $T_{CPA} = t_{cpa} - t_0$, while D_{CPA} indicates the obtainable minimum distance between two aircraft.

B. T_{CPA} and D_{CPA}

Let V_{ij} and P_{ij} be the relative velocity vector and the relative position vector of the two aircraft respectively. Then T_{CPA} and D_{CPA} can be expressed based on the following notations.

We consider that L_1 and L_2 represent the trajectories of two aircraft, $P_i(t)$ and $P_j(t)$ are the associated positions of the two aircraft at time t ,

$$L1 : P_i(t) = P_i^o + V_i * (t - t_0) \quad (1)$$

$$L2 : P_j(t) = P_j^o + V_j * (t - t_0) \quad (2)$$

Since we only consider the process starting from the initial position, thus t_0 is assumed to be 0. Then, the distance between aircraft i and j at time t is given by:

$$\begin{aligned} d_{ij}(t) &= |P_i(t) - P_j(t)| \\ &= |P_i^o - P_j^o + V_i * t - V_j * t| \\ &= |P_i^o - P_j^o + (V_i - V_j) * t| \\ &= |P_{ij} + V_{ij} * t| \end{aligned} \quad (3)$$

When the derivative of $d_{ij}(t)$ with respect to t is equal to 0, the minimum value of $d_{ij}(t)$ is reached. To eliminate the negative values, $D_{ij}(t) = d_{ij}(t)^2$ is used instead of $d_{ij}(t)$.

$$\begin{aligned} D_{ij}(t) &= d_{ij}(t)^2 \\ &= P_{ij}^2 + 2 * P_{ij} * V_{ij} * t + (V_{ij} * t)^2 \end{aligned} \quad (4)$$

The CPA is achieved when the derivative of $D_{ij}(t)$ is 0. Therefore, we calculate the partial derivative of $D_{ij}(t)$ with respect to t .

$$\frac{\partial D_{ij}(t)}{\partial t} = 2 * t * |V_{ij}|^2 + 2 * P_{ij} * V_{ij} \quad (5)$$

$$\frac{\partial D_{ij}(t)}{\partial t} = 0 \quad (6)$$

$$2 * t * |V_{ij}|^2 + 2 * P_{ij} * V_{ij} = 0 \quad (7)$$

$$T_{CPA} = -\frac{P_{ij} * V_{ij}}{|V_i - V_j|^2} \quad (8)$$

We can then determine D_{CPA} :

$$\begin{aligned} D_{CPA} &= d_{ij}(T_{CPA}) \\ &= |T_{CPA} * V_{ij} + P_{ij}| \end{aligned} \quad (9)$$

$$D_{CPA} = \left| -\frac{P_{ij} * V_{ij}}{|V_{ij}|^2} * V_{ij} + P_{ij} \right| \quad (10)$$

These equations of T_{CPA} and D_{CPA} give potential relations among aircraft speeds and positions. In order to detect the effects of inputs on outputs, we present the following model considering all possible encounter situations. In the following work, we will only consider the norm of D_{CPA} .

C. Modeling Formula

Motivated by the goal of developing a model which is beneficial to the sensitivity analysis, the cross point reference coordinate is introduced for this model. This model uses the crossing point of two aircraft trajectories as the center of the coordinate. Two aircraft are located inside an airspace which is shown as a circle, referred to Fig. 2. In this coordinate system, we have the flight direction of aircraft i towards the positive Y axis. We consider that aircraft j only locates in the third and fourth quadrant of our model to avoid the overlap of scenarios and reduce the calculation cost.

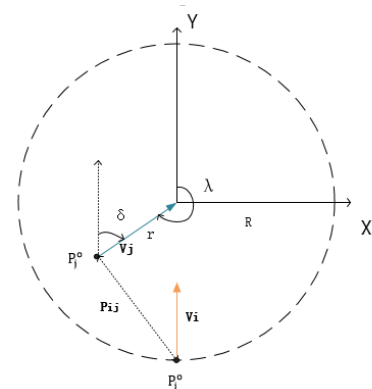


Figure 2. Crossing Point Reference Frame

In this system, we have five variables, namely λ , δ , V_i , V_j , and r . Here we assume:

- The cross point of two trajectories is defined as the origin point of the coordinate.
- The range of radar detection of the aircraft is considered as the distance between aircraft i and the crossing point, the distance is denoted by R which is 74 kilometers.
- r represents the distance between aircraft j and the cross point, $r \in [0, 74km]$.
- Fixed to the Y axis, the heading of aircraft i in the coordinate is towards 0 degree (by definition).
- λ denotes the position azimuth angle of aircraft j . In the model framework, we have the relation between λ and δ : $\lambda = \delta + \pi$.
- Again, V_i and V_j are the speed vectors of aircraft i and j respectively.
- P_i^o and P_j^o are the initial positions of the two aircraft.

Based on these assumptions, this model can suit to any situation when two aircraft are converging by shifting aircraft index i and j . In this framework, the terms related to positions and speeds of the two aircraft are used to compute T_{CPA} and D_{CPA} are presented below:

$$\begin{aligned} P_i^o &= (0, -R) \\ P_j^o &= (r * \sin\lambda, r * \cos\lambda) \\ P_{ij} &= P_j^o - P_i^o = (r * \sin\lambda, r * \cos\lambda + R) \end{aligned} \quad (11)$$

$$\begin{aligned} V_i &= (0, V_i) \\ V_j &= (V_j * \sin\delta, V_j * \cos\delta) \\ V_{ij} &= V_j - V_i = (V_j * \sin\delta, V_j * \cos\delta - V_i) \end{aligned} \quad (12)$$

Using the relation: $\lambda = \delta + \pi$, this model has four variables instead of five. In order to reduce the computational cost, the range of δ is set from 0 to π . As for the speed of aircraft, V_i and V_j vary from 600 km/h to 1000 km/h . Using this model, the scenarios obtained under previous conditions have a large percentage of positive values in terms of T_{CPA} .

Fig. 3 and Fig. 4 show the 3D graph of T_{CPA} and D_{CPA} respectively. The values of T_{CPA} and D_{CPA} are represented by colors. In our equations, the units for the outputs are hour and kilometer for T_{CPA} and D_{CPA} respectively, but when using hour, the scale for T_{CPA} is too small, thus in Fig. 3 we convert it into minute to make the data much easier to show. Since they are 3D figures, only three situations are presented to avoid the overlap of information. Aircraft i has a speed of $|V_i| = 800 \text{ km/h}$ and aircraft j has three different speeds: $|V_j| = 700 \text{ km/h}$, $|V_j| = 800 \text{ km/h}$ and $|V_j| = 900 \text{ km/h}$.

The aim of this paper is to analyze the sensitivity of the T_{CPA} , D_{CPA} when inputs (δ , V_i , V_j , and r) are consisted with uncertainties. In our work, we will make proper choice of sensitivity analysis method considering the parameters and the structure of our model. There are many approaches for sensitivity analysis. For the sake of adapting to our main function, two methods are proposed. One is known as local approach, using partial derivatives to estimate the sensitivity of one specific point. Another one is a variance-based method which is referred as global sensitivity analysis [9].

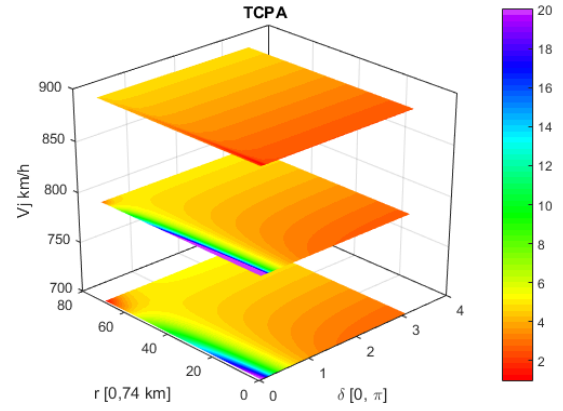


Figure 3. 3D graph of T_{CPA} (min) with different speeds, using color to represent the values of T_{CPA} .

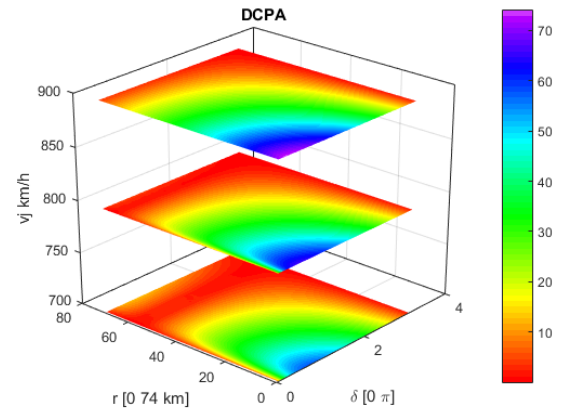


Figure 4. 3D graph of D_{CPA} (km) with different speeds, using color to represent the values of closest distance of two aircraft.

III. LOCAL APPROACH

A. Mathematical Description

This method is widely used to analyze effects of small perturbations of model inputs on model outputs. Local approach is based on partial derivatives [10]. We define the main function as $Y = f(x_1, x_2, \dots, x_k)$ which is a square-integral function. The variables are defined as $X = (x_1, x_2, \dots, x_k)$. The fundamental expression of this method is shown as below:

$$E_i(x^*) = \frac{Y(x_1^*, \dots, x_{i-1}^*, x_i^* + \Delta, x_{i+1}^*, \dots, x_k^*) - Y(x^*)}{\Delta} \quad (13)$$

Where $x^* = (x_1^*, x_2^*, \dots, x_i^*, \dots, x_k^*)$ is the specific point where sensitivity analysis is considered. E_i is the variation of Y with respect to one of its input x_i . We can easily notice that (13) is an equation that shows the partial derivative of the objective function in terms of x_i , so it can be defined as:

$$E_i(x^*) = \frac{\partial Y(x^*)}{\partial x_i} \quad (14)$$

Since our model have considered numerous scenarios, it is difficult to analyze all of them at the same time. However, with the help of Matlab the calculation is achievable and the results can be displayed.

B. Results

With the pre-mentioned formula (8) and (10) in section II and the terms (11) and (12) which derived from the cross point coordinate system, the T_{CPA} and D_{CPA} can be represented by four parameters. We can define T_{CPA} and D_{CPA} as Y , i.e. the outputs of our main function, the variables X will be represented by the current parameters: r , δ , V_i , V_j .

We present four figures to show the evolutions of the two outputs under certain assumptions.

- The speed of aircraft i is fixed at 900 km/h . (Common speed during cruise phase)
- The speeds chosen for aircraft j are 750 km/h and 850 km/h in order to limit the number of figures displayed simultaneously.
- X axis shows the range of δ (heading of aircraft j), Y axis is r (distance between aircraft j and the cross point at the initial point), Z axis shows the exact value of the partial derivative on a given parameter.

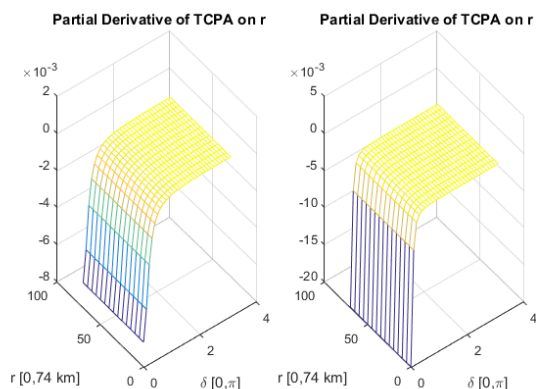


Figure 5. Partial derivative of T_{CPA} with respect to r with different speeds (speeds of aircraft j are 750 km/h for left graph and 850 km/h for the right graph). In the situation with fixed δ , but changing r , the derivative values have minor change. Along with the increase of δ , the influence due to r on T_{CPA} become smaller.

Each figure contains two graphs. The graph on the left side represents the situation that the speed of aircraft j is set to be 750 km/h , the other one represents the situation when the speed of aircraft j is 850 km/h . Fig. 5 and Fig. 6 show the partial derivatives between T_{CPA} and its corresponding variables. Fig. 7 and Fig. 8 provide the same information of D_{CPA} and its variables.

The figures provide us information to analyze the variation trend of T_{CPA} and D_{CPA} according to the partial derivative values derived from each graph. These four figures gather together many situations, among them, the absolute value of partial derivative determines the influence caused by the corresponding variable on the output. When derivative value

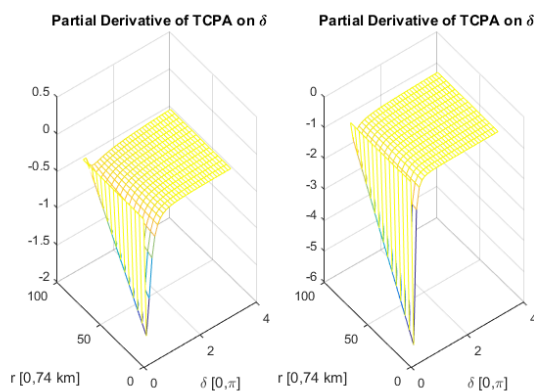


Figure 6. Partial derivative of T_{CPA} with respect to δ with different speeds (speeds of aircraft j are 750 km/h for left graph and 850 km/h for the right graph). When r is small, along with the increase of δ , derivative values have a fluctuation and then become flat. The amplitude of fluctuation decreases with larger r .

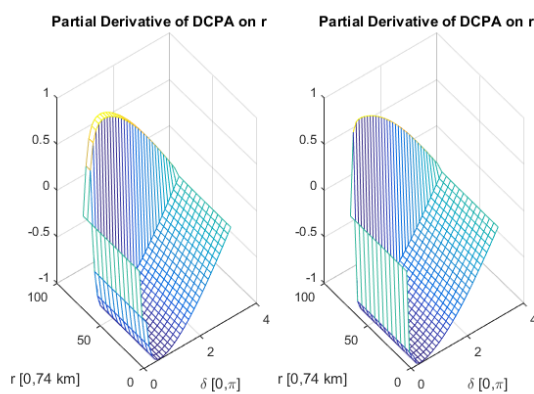


Figure 7. Partial derivative of D_{CPA} with respect to r with different speeds (speeds of aircraft j are 750 km/h for left graph and 850 km/h for the right graph). When δ near 0 and π , the variation of derivative values are small, when δ is around some certain range, along with the decrease of r , the derivative values decrease from positive to negative then become almost flat.

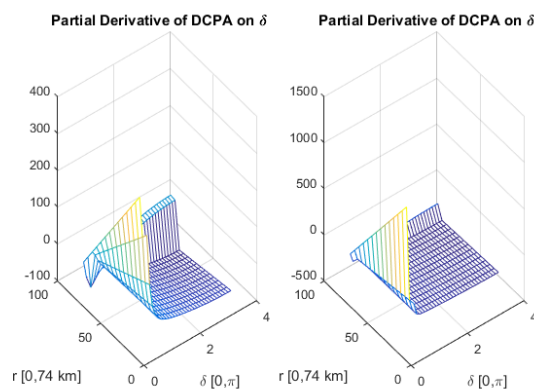


Figure 8. Partial derivative of D_{CPA} with respect to δ with different speeds (speeds of aircraft j are 750 km/h for left graph and 850 km/h for the right graph). Given a fix r , along with the increase of δ , the derivative values have an obvious perturbation at beginning then it tend to be flat.

is near 0, the influence caused by the corresponding variable is relative small. In Fig. 5, since it emphasizes r , so we consider the situation of a given δ , as r changes, the derivatives of T_{CPA} with respect to r is nearly constant. The change of parameter r leads to different influence on T_{CPA} according to δ , when δ is small, r has a relative big influence on T_{CPA} . The same results can be concluded from the other graph in Fig. 5.

Fig. 6 presents the partial derivatives of T_{CPA} with respect to δ . Considering the situation with a small r , such derivatives have a sudden decrease when δ is small, along with the increase of δ , the derivative values approach 0. The variation in graph indicates that δ has a big influential effects on T_{CPA} when it is small, as δ increase, the influence decreases, however, the results are also related to the value of r , when r is large, the influence from δ to T_{CPA} is not obvious, but as r decreases, the influences become more and more strong.

Partial derivatives of D_{CPA} with respect to r and δ are given on Fig. 7 and Fig. 8. The way to analyze the variation trend of D_{CPA} is similar, since those graphs are more complicate, a general conclusion can not be given, the derivative value for a certain scenario can measure the variation of output accurately.

We also notice that the range of derivative values of Fig. 6 is $[-2, 0.5]$ and $[-6, 0]$. In Fig. 5, the ranges correspond to a ratio of 10^{-3} , the scale difference also happens in Fig. 7 and Fig. 8. However, the units of δ and r are different, and we can not tell which inputs gives the most contribution to the output in this case. Through all the graph, the trend for T_{CPA} and D_{CPA} can be analyzed, but without the exact values, this approach can not integrate several inputs for comparison.

The partial derivatives with respect to the corresponding variables exhibits the situation at a given point but it cannot provide a complete and accurate conclusion while it can be done in global sensitivity analysis.

IV. GLOBAL SENSITIVITY ANALYSIS

Global sensitivity analysis is a general method to detect the influential effects from the whole situations [8], so it is possible to get accurate relations between inputs and outputs. There are quite a lot of methods for global sensitivity analysis. These methods can be classified into two main categories: screen technique and variance decomposition. Here are the advantages and drawbacks of these methods.

- Screen technique is usually used in models which have large number of inputs. Due to the relations between inputs and outputs, this method categorizes inputs into several types according to the influence mode and it is usually used with other sensitivity analysis methods in order to deal with huge volume of data. The most typical method is Morris method. However, this kind of methods can not compare the influential values of each input [9][11].
- Variance-based method do not need to know a prior relations between inputs and outputs and it can provide values to compare the effects from inputs to the outputs. Besides, this method is used for non-monotonic and non

linear function. Thus, this method can be chosen for this study.

A. Sensitivity Indices Description

Our main function, $Y = f(x_1, x_2, \dots, x_k)$, is a non-monotonic and non-linear equation, where x denotes the variables and k is the number of variables we have. In our case, the variables are independent. Thus the decomposition of the output variance is validated for variance-based method. The functional decomposition scheme is given as [12]:

$$f = f_0 + \sum_{i=1}^k f_i + \sum_{i=1}^k \sum_{j>i}^k f_{ij} + \dots + f_{12\dots k} \quad (15)$$

The terms inside this equation are related to different variables, $f_i = f_i(x_i)$, $f_{ij} = f_{ij}(x_i, x_j)$ and so on. The unicity of (15) has already been verified [13]. The interpretations of the function are represented as below:

$$\begin{aligned} f_0 &= E(Y) \\ f_i &= E_{x \sim i}(Y | x_i) - E(Y) \\ f_{ij} &= E_{x \sim ij}(Y | x_i, x_j) - f_i - f_j - E(Y) \end{aligned} \quad (16)$$

Where $E(Y)$ denotes the mean expectation of the whole function Y . $E_{x \sim i}(Y | x_i)$ denotes the mean expectation of function Y over all the possible values while keeping x_i fixed and similar meaning for the higher terms.

The decomposition of the variance can be written as follows:

$$\begin{aligned} V_i &= V_{x_i}(E_{x \sim i}(Y | x_i)) \\ V_{ij} &= V_{x_i x_j}(E_{x \sim ij}(Y | x_i, x_j)) \\ &\quad - V_{x_i}(E_{x \sim i}(Y | x_i)) \\ &\quad - V_{x_j}(E_{x \sim j}(Y | x_j)) \end{aligned} \quad (17)$$

Assuming we have k variables. The formula containing all the variance terms can be represented as:

$$V(Y) = \sum_{i=1}^k V_i + \sum_{i=1}^k \sum_{j>i}^k V_{ij} + \dots + V_{12\dots k} \quad (18)$$

If both side are divided by $V(Y)$, we obtain the so called "Sobol's indices":

$$\sum_{i=1}^k S_i + \sum_{i=1}^k \sum_{j>i}^k S_{ij} + \dots + S_{12\dots k} = 1 \quad (19)$$

The first order indices represents the influence which is caused only by a certain variable, denoted by S_i . The total indices of one variable represent the interaction effects of all the inputs, it is noted as S_{T_i} . The way to compute S_{T_i} is S_i plus all the interaction terms which include variable x_i . In this study, the results we extract are the first order indices and the total indices. For other terms, the computational complexity make it hard to decide the second or higher order indices of each input, therefore the results interpretation for these terms are also difficult. The associated sensitivity measurement are written as:

$$S_i = \frac{(V_{x_i}(E_{x \sim i}(Y | X_i)))}{V(Y)} \quad (20)$$

$$S_{T_i} = \frac{(E_{x \sim i}(V_{x_i}(Y | X_{\sim i})))}{V(Y)} \quad (21)$$

B. Monte-Carlo Sampling

The variance-based method consists of two parts. The first part is the data sampling and the second part is the estimator detection.

Monte-Carlo data sampling is a method that provides a series of random data which are compatible with inputs to improve the estimation precision through numerous repetition of calculation.

Two independent sampling matrices A and B with N rows and K columns are generated. N depends on the estimation accuracy that we are targeting for the experiments. Each column corresponding to one input. Two indices i and j refer to the i -th column and j -th row respectively. The index i runs from 1 to N (the number of simulations) and j equals to the number of inputs that we have. Matrix $A_B^{(i)}$ is defined through the way that all columns are from A excepts the i -th column which is from B . An example of matrices recombination is shown in Fig. 9.

| | |
|--|--|
| $\begin{bmatrix} 0.500 & 0.200 & 0.300 & 0.100 & 0.700 & 0.800 & 0.400 & 0.900 \\ 0.500 & 0.200 & 0.300 & 0.100 & 0.700 & 0.800 & 0.400 & 0.900 \\ 0.500 & 0.200 & 0.300 & 0.100 & 0.700 & 0.800 & 0.400 & 0.900 \\ 0.500 & 0.200 & 0.300 & 0.100 & 0.700 & 0.800 & 0.400 & 0.900 \end{bmatrix}$ | $\begin{bmatrix} 0.700 & 0.200 & 0.300 & 0.100 \\ 0.700 & 0.200 & 0.300 & 0.100 \\ 0.700 & 0.200 & 0.300 & 0.100 \\ 0.700 & 0.200 & 0.300 & 0.100 \end{bmatrix}$ |
| A | B |

| | |
|--|--|
| $A_B^{(1)} = \begin{bmatrix} 0.700 & 0.200 & 0.300 & 0.100 \\ 0.700 & 0.200 & 0.300 & 0.100 \\ 0.700 & 0.200 & 0.300 & 0.100 \\ 0.700 & 0.200 & 0.300 & 0.100 \end{bmatrix}$ | |
| $A_B^{(2)} = \begin{bmatrix} 0.500 & 0.800 & 0.300 & 0.100 \\ 0.500 & 0.800 & 0.300 & 0.100 \\ 0.500 & 0.800 & 0.300 & 0.100 \\ 0.500 & 0.800 & 0.300 & 0.100 \end{bmatrix}$ | |
| $A_B^{(3)} = \begin{bmatrix} 0.500 & 0.200 & 0.400 & 0.100 \\ 0.500 & 0.200 & 0.400 & 0.100 \\ 0.500 & 0.200 & 0.400 & 0.100 \\ 0.500 & 0.200 & 0.400 & 0.100 \end{bmatrix}$ | |
| $A_B^{(4)} = \begin{bmatrix} 0.500 & 0.200 & 0.300 & 0.900 \\ 0.500 & 0.200 & 0.300 & 0.900 \\ 0.500 & 0.200 & 0.300 & 0.900 \\ 0.500 & 0.200 & 0.300 & 0.900 \end{bmatrix}$ | |

Figure 9. Matrix Recombination with Monte-Carlo Method

Through the combination of matrices A and B , in each experiment we can change one input for certain times while making other inputs fixed and this explain the principle of variance-based analysis in a way. These matrices will be used in the following calculation in which matrix A and B

and matrix $A_B^{(i)}$ are all used to calculate the corresponding variation or expectation of a certain input to the outputs.

1) *Extraction of probability of failure:* The variables we generate through Monte-Carlo method is uniformly distributed between 0 and 1. Such variable are then transformed to the ranges of the input data of our model. During the process of evaluating T_{CPA} , negative values exist due to some inappropriate situations that have their CPA already passed. We consider it as a kind of probability of failure (P_f) which is caused by the model and Monte-Carlo method:

$$P_f = \bar{I}(\mathbf{X}) = \frac{1}{N} \sum_{k=1}^N I(x_i) = \frac{N_f}{N} \quad (22)$$

Where $\bar{I}(\mathbf{X})$ is the expected value of all $I(\mathbf{X})$, $I(\mathbf{X})$ refers to an indicator function, which is defined as:

$$I(\mathbf{X}) = \begin{cases} 1 & \text{if } Y(x) \leq 0 \\ 0 & \text{otherwise} \end{cases} \quad (23)$$

In our case, the number of experiments is 10^5 . According to the reference, the probability of failure experiments extracted from the Monte-Carlo simulation is around 4% to 5%. Such percentage of failure is small, we can consider that our computation process is still effective.

2) *Estimator:* The estimators of "Sobol's indices" are based on the sensitivity indices. The expression of estimators have already been validated by lots of experts.

With the matrix established, $V_{x_i}(E_{x \sim i}(Y | x_i))$ contributes to calculate the first order effect for S_i and $E_{x \sim i}(V_{x_i}(Y | x_{\sim i}))$ contributes to S_{T_i} [14] e.g.:

$$V_{x_i}(E_{x \sim i}(Y | x_i)) = \frac{1}{N} \sum_{j=1}^N f(B)_j (f(A_B^{(i)})_j - f(A)_j) \quad (24)$$

$$E_{x \sim i}(V_{x_i}(Y | x_i)) = \frac{1}{2N} \sum_{j=1}^N (f(A)_j - f(A_B^{(i)})_j)^2 \quad (25)$$

Based on the data sampling, the generated data can be applied in the estimators to generate the matrices that are used in (24) and (25), thus the first order indices (S_i) and total indices (S_{T_i}) can be computed.

C. Results

Here, we note that (19) indicates that the sum of indices equals to 1. Since we have four variables, thus we consider that for an input whose first order indices is bigger than 0.3 has a big influential effect on the output. The main functions of sensitivity analysis are $T_{CPA} = f(\delta, r, V_j, V_i)$ and $D_{CPA} = f(\delta, r, V_j, V_i)$.

The property of Monte-Carlo method makes the generated data change every time, hence the results for each experiment have slightly differences. Through a probabilistic way, the results that we get can reflect the contribution from each input to the output.

TABLE I
FIRST ORDER EFFECTS OF T_{CPA}

| $S_1(\delta)$ | $S_2(r)$ | $S_3(V_j)$ | $S_4(V_i)$ |
|---------------|----------|------------|------------|
| 0.6784 | 0.0171 | 0.0411 | 0.0178 |
| 0.6813 | 0.0139 | 0.0455 | 0.0159 |
| 0.6809 | 0.0221 | 0.0435 | 0.0143 |
| 0.6873 | 0.0084 | 0.0440 | 0.0170 |
| 0.6727 | 0.0182 | 0.0402 | 0.0186 |

TABLE II
TOTAL EFFECTS OF T_{CPA}

| S_{T1} | S_{T2} | S_{T3} | S_{T4} |
|----------|----------|----------|----------|
| 0.9284 | 0.2721 | 0.0535 | 0.0210 |
| 0.9171 | 0.2711 | 0.0539 | 0.0211 |
| 0.9249 | 0.2689 | 0.0540 | 0.0210 |
| 0.9235 | 0.2742 | 0.0543 | 0.0212 |
| 0.9208 | 0.2715 | 0.0538 | 0.0212 |

TABLE III
FIRST ORDER EFFECTS OF D_{CPA}

| $S_1(\delta)$ | $S_2(r)$ | $S_3(V_j)$ | $S_4(V_i)$ |
|---------------|----------|------------|------------|
| 0.3465 | 0.4109 | 0.0440 | 0.0413 |
| 0.3482 | 0.4120 | 0.0431 | 0.0443 |
| 0.3447 | 0.4137 | 0.0456 | 0.03995 |
| 0.3529 | 0.4004 | 0.0422 | 0.0428 |
| 0.3441 | 0.3968 | 0.0441 | 0.0428 |

TABLE IV
TOTAL EFFECTS OF D_{CPA}

| S_{T1} | S_{T2} | S_{T3} | S_{T4} |
|----------|----------|----------|----------|
| 0.4877 | 0.7077 | 0.0939 | 0.0919 |
| 0.4837 | 0.7020 | 0.0950 | 0.0919 |
| 0.4835 | 0.7092 | 0.0945 | 0.0925 |
| 0.4838 | 0.7060 | 0.0942 | 0.0920 |
| 0.4836 | 0.7015 | 0.0935 | 0.0911 |

Tab. I displays the first order effects of each input to T_{CPA} , while in Tab. II, total effects are represented. Regarding to the relative connections between variables and the indices, we can get the conclusion as follows:

For first order effects of T_{CPA} , we have $S_1 > S_3 > S_2 \approx S_4$ while the total effects have the order of $S_{T1} > S_{T2} > S_{T3} > S_{T4}$. Regarding the corresponding variables, the rank of inputs due to influential effects is $\delta > V_j > r \approx V_i$. Taking the first order indices and total effects into consideration, the relative contribution from inputs to outputs should be approximately determined.

In this case, δ obtains the highest influence in affecting the output itself and other inputs have absolutely small effect compare to δ . Referring to the method provided in [15], when the order of the total effects are different from the first-order indices, the inputs which have relative high difference on the indices will be compared. In our case, r (the distance between aircraft j to crossing point, more intuitively can be thought as the relative position of two aircraft) does not obtain a high value on the first order indices, however it has a strong effect on the output together with other inputs. So r is also a parameter which should be considered seriously. Thus, in reality and in the aspect of time, relative flight direction of two aircraft (δ) should be first considered in case of conflict and the relative position of the aircraft (r) can be taken as a reference to avoid the emergency situation.

Tab. III and Tab. IV indicate the potential sensitivity of variables and the closest distance between two aircraft. Both the first order indices and the total effects have the same order of $r > \delta > V_i \approx V_j$. r is the key parameter while relative flight direction of two aircraft (δ) is also important in affecting the closest distance of two aircraft.

The sensitivity analysis of T_{CPA} and D_{CPA} demonstrates that during the convergence of two aircraft, the key parameters are relative flight direction of two aircraft and the distance between aircraft j to cross point. The speeds of two aircraft have a relative small effect. The proposed methodology will help the investigation of aircraft movement and encounter status and it is beneficial to facilitate the emergency strategies and ensure the safety for air traffic management and also can be used in the route design process.

V. CONCLUSION

The main objective of this paper is to use appropriate method to support sensitivity analysis of CPA. All the work that have been done in this paper relies on the mathematical computation formula of T_{CPA} and D_{CPA} . The proposed model is compatible to the sensitivity analysis and satisfy the condition of including all possible scenarios.

The sensitivity analysis method presented in this paper can either detect the sensitivity of one specific point or from a general perspective. The key point of using local approach is the existence of partial derivative from the main function with respect to the corresponding variables. Variance-base method is using Monte-Carlo method to generate uniformly distributed data for the matrices, the calculated results for each experiment turn out to be really close to each other.

In this paper the speeds of aircraft, the distance from cross point to the position of aircraft j and the heading of aircraft have been introduced to describe the scenarios. With all these hypotheses, a scenario with two converging aircraft can be found in the model. Local approach enable to analyze the variation of outputs for a specific situation, while variance-based method explains the influential effects from inputs to the outputs as a whole.

The sensitivity analysis is useful for quantifying the performance of resolution methodologies. The future step is to

establish the same relations for a 3 dimension model as well as considering the uncertainty of wind or other weather conditions.

ACKNOWLEDGEMENT

The author is gratefully acknowledge the support of Mr. Serge Roux for his assistance with technical improvements.

REFERENCES

- [1] Alam S, Shafi K, Abbass H A, et al. Evolving air traffic scenarios for the evaluation of conflict detection models[C]//Proc. 6th Eurocontrol Innovative Research Workshop, Eurocontrol Experiment Research Center. 2007.
- [2] Kuchar J K, Yang L C. Survey of Conflict Detection and Resolution Modeling Methods[C]. AIAA Guidance, Navigation, and Control Conf. 1388-1397.
- [3] Munoz C, Narkawicz A, Chamberlain J. A TCAS-II resolution advisory detection algorithm[C]. Proceedings of the AIAA Guidance Navigation, and Control Conference and Exhibit. 2013.
- [4] Sensitivity analysis[M]. New York: Wiley, 2000.
- [5] Houck S, Powell J D. A parametric sensitivity study of ultra closely spaced parallel approaches[C]. Proceedings of the Digital Avionics Systems Conference, Philadelphia, PA. 2000.
- [6] Jackson M R, Zhao Y J, Slattery R A. Sensitivity of trajectory prediction in air traffic management[J]. Journal of Guidance Control and Dynamics, 1999, 22: 219-228.
- [7] Arumugam S, Jermaine C. Closest-point-of-approach join for moving object histories[C]. Data Engineering, 2006. ICDE'06. Proceedings of the 22nd International Conference on. IEEE, 2006: 86-86.
- [8] Kucherenko S. Derivative based global sensitivity measures and their link with global sensitivity indices[J]. Mathematics and Computers in Simulation, 2009, 79(10): 3009-3017.
- [9] Bertrand Iooss, Paul Lematre. A review on global sensitivity analysis methods. C. Meloni and G. Dellino. Uncertainty management in Simulation-Optimization of Complex Systems: Algorithms and Applications, Springer, 2015.
- [10] Kucherenko S., Iooss B. (2015) Derivative-Based Global Sensitivity Measures. In: Ghanem R., Higdon D., Owhadi H. (eds) Handbook of Uncertainty Quantification. Springer, Cham
- [11] Campolongo F, Cariboni J, Saltelli A, et al. Enhancing the Morris method[C]. Sensitivity Analysis of Model Output. Proceedings of the 4th International Conference on Sensitivity Analysis of Model Output (SAMO 2004). 2005: 369-379.
- [12] Homma T, Saltelli A. Importance measures in global sensitivity analysis of nonlinear models[J]. Reliability Engineering System Safety, 1996, 52(1): 1-17.
- [13] M. Sobol, I. (1993). Sensitivity analysis for non linear mathematical model. Mathematical Modeling and Computational Experiment 1(1993) 407-414.
- [14] Saltelli A, Annoni P, Azzini I, et al. Variance based sensitivity analysis of model output. Design and estimator for the total sensitivity index[J]. Computer Physics Communications, 2010, 181(2): 259-270.
- [15] Jacques J, Lavergne C, Devictor N. Sensitivity analysis in presence of model uncertainty and correlated inputs[J]. Reliability Engineering System Safety, 2006, 91(10): 1126-1134.